THE JOURNAL OF PHYSICAL CHEMISTRY B

B: Biophysics; Physical Chemistry of Biological Systems and Biomolecules

Effect of the Organization of Rhodopsin on the Association Between Transducin and a Photoactivated Receptor

Samuel Andres Ramirez, and Chad Leidy

J. Phys. Chem. B, **Just Accepted Manuscript** • DOI: 10.1021/acs.jpcb.8b07401 • Publication Date (Web): 29 Aug 2018

Effect of the Organization of Rhodopsin on the Association Between Transducin and a Photoactivated Receptor

Samuel A. Ramirez [†*] *and Chad Leidy* [‡]

[†]Department of Pharmacology, University of North Carolina at Chapel Hill, Chapel Hill, North Carolina, 27599; [‡] Department of Physics, Universidad de los Andes, Bogotá, Colombia, 111711

[*] Correspondence: samurami@gmail.com

ABSTRACT: After photoactivation, rhodopsin (R), a G-protein-coupled receptor, rapidly activates multiple transducin G-proteins (G) in an initial amplification step of phototransduction. G-protein activation requires diffusion mediated association with an active rhodopsin (R*) at the rod disc membrane. Several microscopy studies have revealed different organizations of R within the membrane, including static and freely diffusing situations. However, it is unclear how such different scenarios influence the activation rate of G proteins. Through Monte Carlo simulations, we study the association reaction between a photoactivated rhodopsin (R*) and transducin under different reported receptor organizations including: a) R monomers diffusing freely, b) R forming static, dispersed crystalline domains made of rows of dimers, and c) R arranged in static tracks formed by two adjacent rows of dimers. We perform simulations varying the probability of binding following a collision (*p*). For high *p*, the association rate between R* and G is higher in the freely diffusive system than in the static organizations, but for low collision efficiencies, the static organizations can result in faster association rates than the mobile system. We also observe that with low *p*, increasing the concentration of R increases the association rate significantly in the dispersed crystals configuration and just slightly in the free diffusive system. In summary, the lateral organization of rhodopsin influences the association rate between R* and G in a manner strongly dependent on the collision efficiency.

INTRODUCTION

At night, our visual system can resolve signals as weak as a few photons per second. Two of the requirements to achieve this outstanding sensitivity are a high efficiency of photon capture at rod photoreceptor cells, and subsequent amplification of this event into a significant electrical signal in the rod cell [1]. Photons are absorbed by rhodopsin (R), a G-protein-coupled receptor found at high concentration at the membrane of the discs in the rod outer segment. The elevated number of rhodopsin molecules in the discs accounts for an efficient photon capture. Upon absorption of a photon, R becomes activated and triggers a cascade of reactions that results in photoresponse amplification. The first step in this cascade, crucial for signal amplification, is the rapid activation of many G-protein transducins (G) by a photoactivated rhodopsin (R*). Transducin activation requires the lateral encounter and binding between G and R*, and the subsequent exchange of GDP for GTP in the alpha subunit of transducin mediated by R*.

Early research on phototransduction proposed that rhodopsin molecules within the disc membrane existed as monomers that underwent rapid lateral diffusion [2,3]. Such observations prompted researchers to hypothesize that the fast lateral diffusion of rhodopsin was essential for the rapid encounters between R* and G required for fast G activation. However, more recent experiments using atomic force microscopy, electron microscopy, and biochemical approaches [4–10] have revealed that rhodopsin can be found on the disc membrane as static dimers forming oligomeric structures also called nanodomains. Furthermore, a reappraisal of the lateral diffusion of rhodopsin indicates that there is a fraction of immobile receptors that can vary between zero and 100%, and it is likely that the immobile fraction corresponds to receptors forming nanodomains [11,12]. These observations have motivated a re-evaluation of the effect of R mobility and organization on the initial steps of phototransduction [12,13].

Computational studies have concluded that a static configuration of R is still compatible with the rapid activation of G proteins, as the fast diffusion of transducin can account for a high frequency of lateral encounters with an immobile R [10,14,15]. Such studies have also suggested that scenarios with static R result in a slower rate of G activation compared with situations where R*

can diffuse. Using Monte Carlo simulations on a discrete grid, Dell'Orco and Schmidt [14] looked at the first encounter time between a single R* and transducin molecules. They observed that for a high concentration of R, an organized static configuration of dimeric receptors results in faster first-encounters compared to a scenario with unorganized static rhodopsin. Nevertheless, allowing R to freely diffuse, while maintaining the diffusivity of G at its physiological value will result in faster first encounter times compared to the static organized configuration due to higher overall mobility in the freely diffusive scenario. Schoneberg et al. 2014 used a Brownian dynamics approach to model the different steps that lead to the activation of transducin upon activation of a single R [15]. Their simulations suggested that an organization where inactive dimeric rhodopsins form static compact racks while the activated receptor can diffuse freely, results in a similar rate of G activation as the case where all receptors diffuse in monomeric form. However, if R* forms part of a rack, the activation rate of G is significantly reduced compared to the freely diffusing scenario. In a subsequent study, Gunkel et al. 2015 described experimentally and simulated a configuration where R is organized in tracks made of two adjacent rows of dimers [10]. They also observed that a freely diffusive scenario yields a faster encounter rate than the tracks configuration. Overall, these studies observed faster R*-G first encounters in a free diffusive system compared to a static R* situation, and this can result in faster G activation in the mobile system. However, in a setting where the probability of association between R* and G following an encounter is low, in addition to the frequency of first encounters, re-encounters may also influence the rate of G activation [16,17].

Here we perform Monte Carlo simulations of the diffusion mediated association between R* and G at the disc membrane. In our simulations transducin binds R* with probability *p* upon collision. Furthermore, a binding event can occur only when G collides with R* at certain positions (active sites), which reflects better the physiological situation. We consider three organizations of rhodopsin in the membrane: a) the classic view where rhodopsin molecules diffuse as monomers, b) a system where rhodopsin is found as static dispersed crystals made of rows of dimers and c) an organization where rhodopsin is arranged in static tracks made of 2 adjacent rows of dimers. We observe that, compared to the freely diffusive configuration, the static organizations of receptors can result in higher, lower or similar association rates between R* and G, with the outcome depending on the collision efficiency *p*.

METHODS

Monte Carlo simulations were carried out in a triangular grid (rhombus shaped domain) with periodic boundary conditions and lattice size Δx = 1.2nm. In this setting pixels are rhombi with area $3^{1/2}\Delta x/2$. R monomers and G proteins were represented by hexagonal arrays of 7 and 19 pixels respectively (Fig 1 b) resulting in an effective protein size of 3nm for R and 5nm for G, which are values close to physiological estimates [18,19]. Rhodopsin is a transmembrane protein and transducin is a peripheral protein anchored to the membrane by means of lipid modifications in its alpha and gamma subunit. This allows G to protrude farther away from the membrane leading to an umbrella-like overlap between R and G when these two proteins approach each other [20]. To account for this difference in the positioning at the membrane in our simulations, G proteins can partially overlap with rhodopsin proteins as shown in Fig. 1 *b*. For simplicity, we represented just one lipid modification of transducin as a pixel at the center of the protein, and this anchor cannot overlap with R following Dell'Orco and Schmidt 2008 [14]. We tracked the number of binding events between an R* and different transducin molecules. Once a particular G has reacted, it keeps diffusing but cannot bind the same photoactivated receptor again. To avoid artificial effects due to depletion of G as they react, we selected the size of the grid so that no more than 7% of the pool of transducins react with an R* during a simulation. Following this criterion, the side L of the grid was ~1μm.

Rhodopsin supramolecular configuration. As described in the introduction, rhodopsin can form higher order structures made of rows of stacked dimers in the disc membrane. We represent a dimer with two adjacent hexagonal rhodopsins resulting in a separation between monomer centers of ~3.2nm (Fig. 1 d). Dimers are set in three possible orientations that follow from rotations without considering mirror reflections (Figs. 1 c, 1 d). Rows were made of stacked dimers such that G proteins can diffuse across rows [10,14].

Separate studies have reported different configurations of the rows of dimers. Here we simulate the following representative organizations: a nanodomains scenario with dispersed crystals each one made of rows aligned next to each other, a configuration with dispersed tracks

each one formed by 2 adjacent rows of dimers [10], the classic scenario where monomers of rhodopsin freely diffuse, and a configuration with immobile rhodopsin monomers randomly located in the membrane. To generate the dispersed crystals configuration, we first allocate a number of dimers at random locations and with random orientations. These dimers act as nucleation seeds for the crystals. To grow the crystals, a seed is selected arbitrarily and one dimer is added in a randomly selected position along the perimeter of the growing crystal. The growth process continues until a specified fraction of area covered by rhodopsin (*f*) is reached. We used a density of 593 seeds/μm^2, so that at full coverage of receptors, we obtain an arrangement qualitatively similar to the compact arrangement reported by Fotiadis et al. in 2003 [8]. The tracks configuration is generated with an analogous crystal-growing procedure as before, but seeds are track units: 2 dimers, each one belonging to one of the rows forming the track. Such seeds are then randomly added in either the front or the back of the growing track. We adjusted the number of seeds in this case to obtain a particular average track length at the physiological concentration of R. Gunkel et al., 2015 reported a minimum length of 10 dimers in a row per track. We ran simulations with average lengths of 10, 15, and 20 dimers in a row per track. The kinetics were similar in each of these cases (Supporting Information).

Random walk simulations. For every time step, every mobile protein in the simulations is selected and allowed to move one step Δx with probability p_{jump}. The direction of the movement is selected randomly from the six possible directions on the grid. If there is an obstruction in the new position of the protein the jump is rejected. We determined the effective diffusion coefficient of a protein as:

$$D_{eff} = \frac{\langle r^2 \rangle}{4t_f}$$

where $\langle r^2 \rangle$ is the mean squared displacement for a time interval of t_f = 60ms. In the absence of obstructions, the effective diffusion coefficient is known to be $D_{\text{max}} \times p_{\text{jump}}$, where $D_{\text{max}} = \Delta x^2/(4\Delta t)$. We used a time step Δt = 0.18μs so that D_{max} = 2μm^2/s. However, in the presence of obstacles (e.g. other proteins in the membrane), the effective diffusion coefficient will be less than $D_{\text{max}} \times p_{\text{jump}}$. We adjusted p_{jump} so that the effective diffusion coefficients in the monomeric diffusive configuration matched the experimentally determined values at physiological concentrations of R and G. In this case, the concentrations of R and G are 25000/μm^2 and

2500/μm^2 respectively, and the effective diffusion coefficients are $D_R \sim 0.4\mu m^2/s$ for rhodopsin [11] and $D_G \sim 1.0\mu m^2/s$ for transducin [21]. The adjusted values of p_{jump} were 0.34 for R and 0.75 for G. These parameters were not modified in our simulations, except for the configurations where rhodopsin is static, in this case $p_{jump} = 0$ for R. The number of trajectories used to estimate D_{eff} varied between ~130000 and ~500000 for R and between ~20000 and ~30000 for G.

Simulation of reactions. Upon a collision, G and R* can bind with probability *p* (collision efficiency). Once a transducin has participated in a binding event it remains diffusing on the grid but can no longer react with the same R*. We count a collision when one protein, or both, attempt to jump into the grid points occupied by the other protein, and the center of G is located in one of the active sites around R* (Fig. 1 *b*, *d*). The reaction is tried with probability *p* if the center of G is still in an active site after both proteins attempted to move during a timestep of the simulation. This is to avoid reactions when one protein jumps towards the other, but the later jumps away from the former during the same Δt. We consider a limited number of active sites for R* to reflect the fact that G must approach a rhodopsin molecule from a particular direction in order to bind it [20]. In the main text we present results using 5 active sites. Changing this parameter does not change our conclusions as shown in the Supporting Information.

Association rate constant *k*. We estimated *k* from the average rate of binding events N_{bind} after t_f = 60ms as :

$$k = \frac{\langle N_{bind} \rangle}{t_f [G]}$$

where [G] is the concentration of G (2500/μm^2).

The first-encounter rate is calculated as $\langle N_{bind} \rangle / t_f$ from simulations where G binds R* immediately once they are in proximity.

To increment the data acquisition in a single simulation, multiple rhodopsins are randomly labeled as R*. The binding reactions are tracked independently for each R* without crosstalk between R*s: a G protein that has bound a particular R* but has not reacted with a second one, can bind the second R*. For the monomeric diffusive and random static distributions, *k* was

estimated from a total number N_{R^*} = 20000 of activated receptors. For the dispersed crystals and tracks configurations N_{R^*} = 10000. The standard error of *k* was computed as:

$$\mathrm{SE}(k) = \frac{\mathrm{SD}(N_{bind})}{t_f[G]N_{R*}^{1/2}}$$

where SD(N_{bind}) is the standard deviation of N_{bind}.

Diffusive and reactive rate constants (k_D and k_r). These rates were obtained from a fit to the data of 1/k vs. 1/p as shown in Fig. 2, b. The statistical error in the values of k_D and k_r was obtained from the standard deviation of three independent estimations.

Software and performance. The simulations were implemented in C++, the code is available upon request. The CPU time for a simulation of 60ms depended on the setting. When run on a computer with 32GB memory and 3.5 GHz Intel Core i7 processor, a typical simulation with a static rhodopsin configuration took ~210s CPU time, and for a free diffusing scenario this time varied between 670s and 2700s depending on the concentration of receptors.

RESULTS AND DISCUSSION

By means of Monte Carlo simulations we studied how the organization of rhodopsin in the membrane affects the association reaction between a single photoactivated rhodopsin and transducin molecules. First we considered a scenario where rhodopsin molecules are found as monomers that diffuse freely in the membrane (Fig. 1, *a* and *b*), and a configuration where the receptors form dispersed static crystals made of rows of dimers (Fig. 1, *c* and *d*). We simulated the lateral diffusion of G proteins (and rhodopsin molecules in the monomeric diffusive scheme) in a triangular grid (Fig. 1, *b* and *d*). In our simulations a binding event will occur with probability *p* upon collision between R* and transducin (see Methods). We estimate the rate constant *k* of the association reaction between a single R* and G as the rate of average binding events (Fig. 2 *a*) divided by the concentration of transducin.

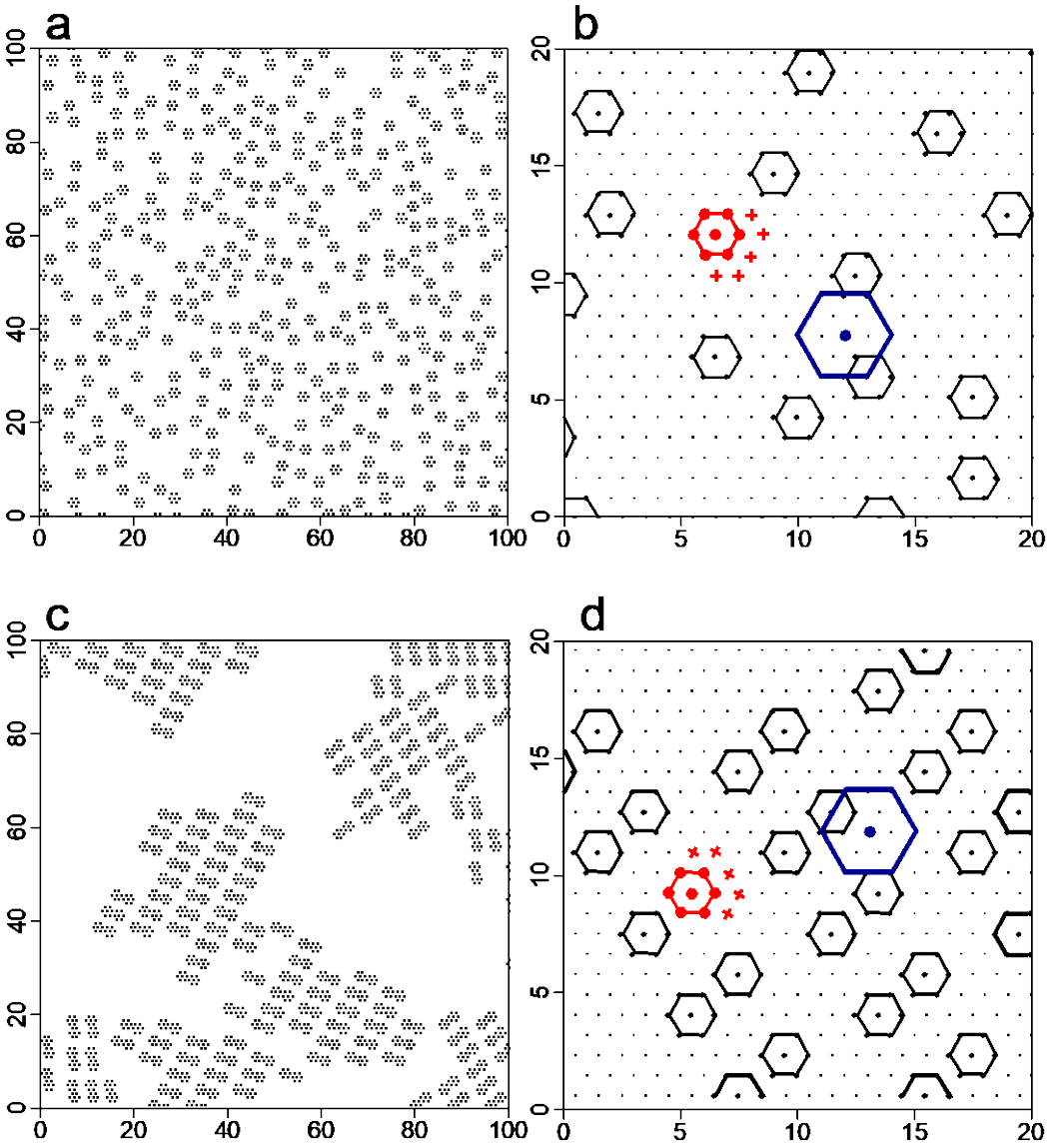

FIGURE 1 Representation of rhodopsin and transducin molecules on the triangular grid. (*a*) Monomeric diffusive scheme. (*b*) Magnification of a region of the area in *a* showing individual rhodopsin monomers. We also include a transducin shown as a blue hexagon and a photoactivated rhodopsin shown as a red hexagon. Red crosses indicate the active sites of the photoactivated rhodopsin. (*c*) Example of the arrangement of rhodopsin molecules in the dispersed crystals scheme. A crystal is made of adjacent rows of dimers with the same orientation. (*d*) Magnification of a region of the area in *c* showing individual dimers of R stacked in rows. A transducin, a photoactivated R and the active sites of R* are shown with the same format as in *b*. *a* and *c* are patches from grids containing the physiological concentration of R.

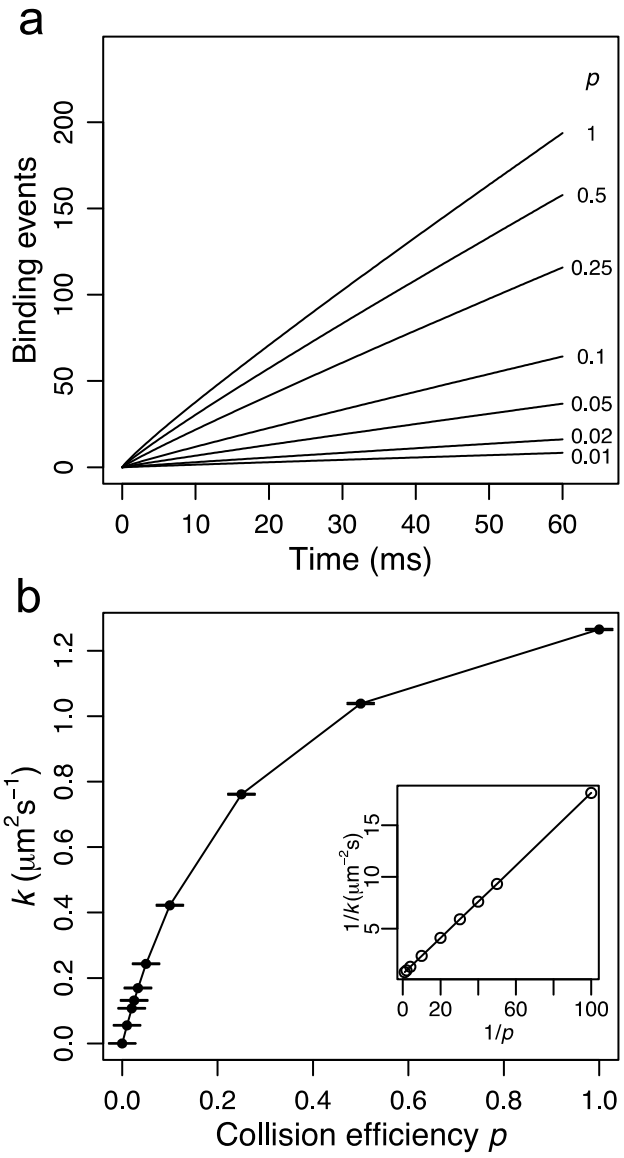

FIGURE 2 Estimation of the association rate constant k, the diffusive rate constant k_D and the reactive rate constant k_R. (*a*) The time series of average binding events between G and R* shows a linear trend for each value of the collision efficiency p simulated. This shows that the change in abundance of G during a simulation is not significant enough to affect k dramatically. (*b*) The association rate constant k is calculated as the average binding events at t = 60 ms divided by the concentration of G and t, and is plotted as a function of the collision efficiency p. Error bars are ± 2 SE. Inset: Eq. 1 was fit to the data in *b* to determine the first-encounter rate constant k_D and the reactive rate constant k_R. In this case, the rate constants were calculated to be $k_D = 1.63$ $\mu m^2 s^-$

[1] and k_R = 5.72 $\mu m^2 s^{-1}$. The data corresponds to simulations of the free diffusing scenario at physiological concentration of rhodopsin and transducin (25000/μm^2 and 2500/μm^2 respectively).

The association rate, *k*, is higher in the freely diffusive system than in the dispersed crystals configuration when the collision efficiency is high (Fig. 3 *a*). In this regime, a faster rate of first-encounters in the monomeric diffusive configuration compared to the dispersed crystals system (Fig. 3. *B*) results in a higher association rate in the former than in the later arrangement. The higher first-encounter rate in the freely diffusive system is expected due to a higher total diffusivity ($D = D_R + D_G$ = 1.4μm^2/s) as compared to the static configuration where only G diffuses (D = 0.91μm^2/s). However, for low collision efficiencies, the association rate is faster in the dispersed crystals configuration compared to the monomeric diffusing scenario (Fig. 3 *a*). In this case, a binding event is not likely to occur upon an initial encounter between R* and G, however, a higher probability of recollision in the dispersed crystals configuration (Fig. 3 *c*) increases the chance of binding between two molecules that are in close proximity, therefore enhancing the association rate [16,22].

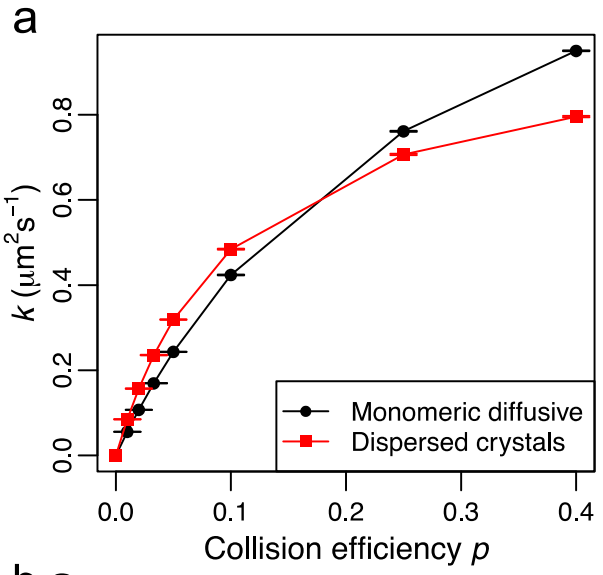
a
k (μm²s⁻¹)
0.0
0.2
0.4
0.6
0.8
0.0
0.1
0.2
0.3
0.4
Collision efficiency p
Monomeric diffusive
Dispersed crystals

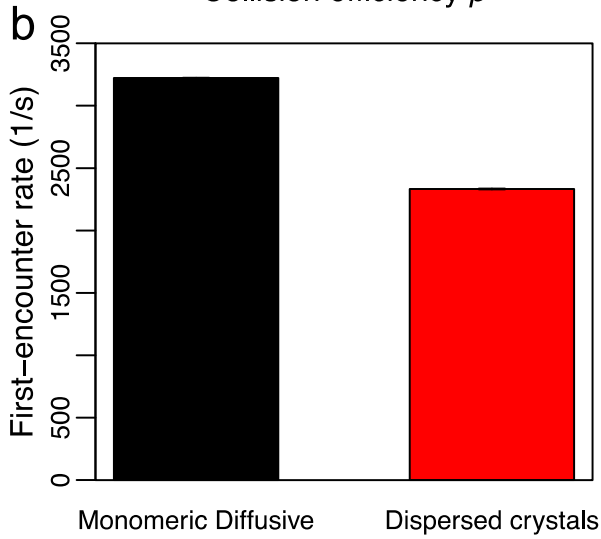
b
First−encounter rate (1/s)
0
500
1500
2500
3500
Monomeric Diffusive
Dispersed crystals

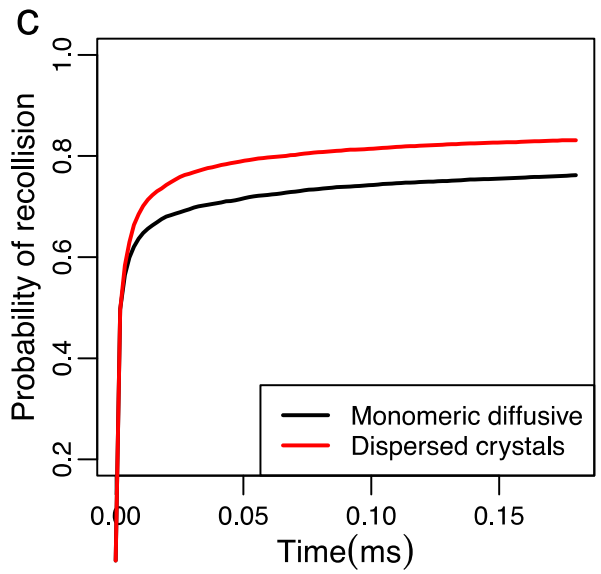
c
Probability of recollision
0.2
0.4
0.6
0.8
1.0
0.00
0.05
0.10
0.15
Time(ms)
Monomeric diffusive
Dispersed crystals

FIGURE 3 The value of the collision efficiency *p* determines which organization of rhodopsin results in a faster association kinetics. (*a*) The association rate constant *k* is plotted as a function of the collision efficiency *p* for the monomeric diffusive and dispersed crystals organizations of rhodopsin. Error bars are ± 2 SE. (*b*) First-encounter rate for the monomeric diffusive and dispersed crystals configurations, the standard errors are 1.5/s and 5.7/s respectively. (*c*) The re-encounter time is tracked for 10000 collision events and the probability of recollision is plotted as a function of time for both scenarios. The simulations are performed using the physiological concentration of R.

The contribution of the first-encounters and recollisions to the association rate can be expressed quantitatively as:

$$\frac{1}{k} = \frac{1}{k_D} + \frac{1}{p \times k_R} \qquad (1)$$

where k_D is a diffusive rate constant related to the first-encounter rate between reactants and k_R is a reactive constant related to the probability of recollision upon an unreactive collision [17]. Equation (1) shows in mathematical form how the collision efficiency *p* modulates the contribution of k_D and k_R to the association rate. Furthermore, these constants can be determined by fitting Eq. 1 to our association rates data (for example see Fig. 2 *b* and inset). To better understand how the organization of rhodopsin influences the association rate constant *k* by separately influencing first-encounters and recollisions, we show below how k_D and k_R behave for different configurations and concentrations of the receptors.

For all R concentrations tested, the diffusive rate constant k_D is higher in the monomeric diffusive system compared to the dispersed crystals configuration (Fig. 4 *a*). This is in agreement with a higher first-encounter rate (Fig. 3 *b*) due to the higher mobility in the freely diffusive system. For higher concentrations of R, *D* decreases due to obstruction effects (Fig. 4 *c*) and consequently the reactive constant k_D is reduced in both configurations (Fig. 4 *a*). The change in k_D, however, is more gradual in the dispersed crystals scheme than in the freely diffusing system (Fig. 4 *a*). This observation is in part explained by a similar trend for the total diffusion (Fig. 4

c), where *D* decreases slower in the dispersed crystals configuration than in the monomeric diffusive system with higher levels of R.

To investigate how the particular organization of R in the dispersed crystals scenario influences k_D, we also ran simulations for a static non-crystallized configuration where R monomers are randomly allocated and remain immobile (Fig. 4 *a*, *open circles*). This configuration results in a diffusion coefficient ($D = D_G$) comparable to the dispersed crystals organization at moderate concentrations of R (Fig. 4 *c*). Interestingly, k_D is lower in the dispersed crystals configuration compared to the static random scheme at low concentrations of R, despite having a similar or higher *D* (compare Fig. 4 *a* and *c*). The reduced k_D in the dispersed crystals configuration is likely related to the clustering of rhodopsin molecules into oligomeric structures, which hampers the arrival of new G proteins to the photoactivated receptor. In contrast, the static random configuration is characterized by R proteins with no neighbors, and this arrangement facilitates first encounters between R* and G for low levels of R. As we increase the concentration of R, however, k_D is no longer higher in the static random arrangement compared to the dispersed crystals configuration; in agreement with [14], the organized static configuration results in higher diffusive rate constant than the unorganized scheme. This is a consequence of a greater reduction in protein mobility in the random static scenario than in the dispersed crystals configuration as the levels of R increase (Fig. 4 *c*). We note that even at the highest density of R shown here, the static random configuration is at a concentration below the percolation threshold [23], therefore, the reduction in k_D is attributed mainly to a reduction in the normal diffusion due to obstacles and not due to trapping of G proteins in finite regions bounded by receptors.

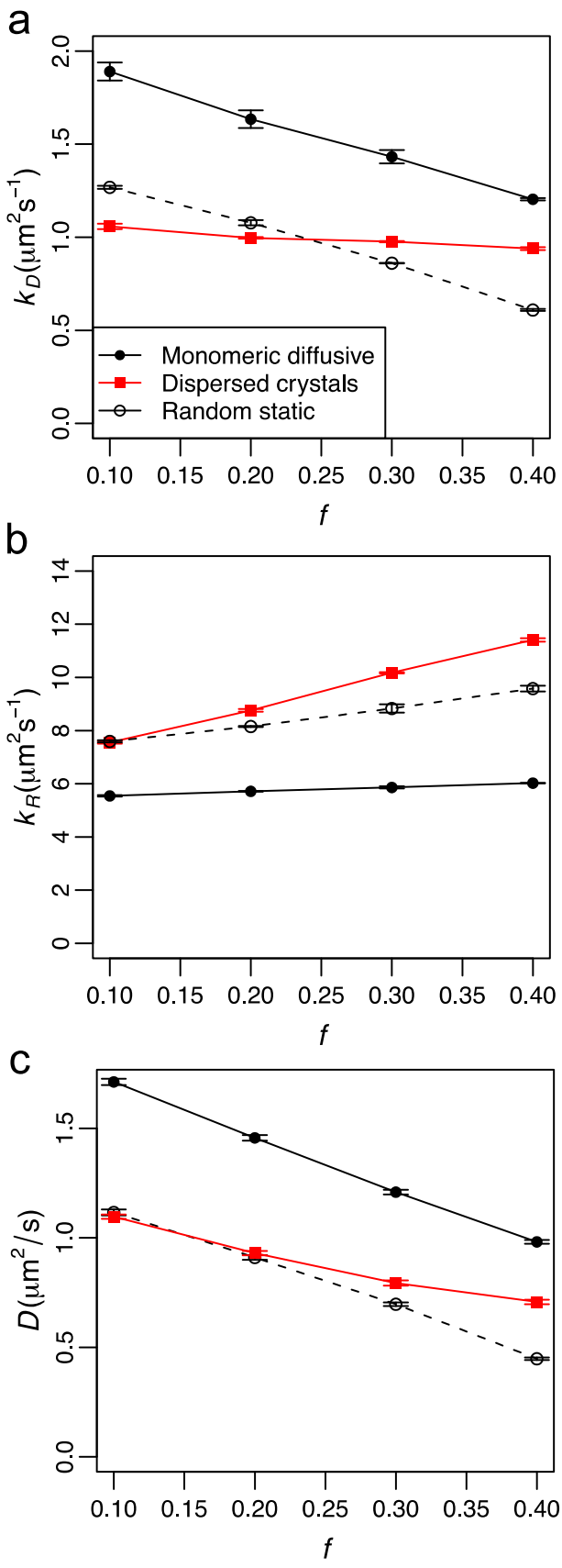
a
$k_D(\mu m^2 s^{-1})$
0.0
0.5
1.0
1.5
2.0
Monomeric diffusive
Dispersed crystals
Random static
0.10 0.15 0.20 0.25 0.30 0.35 0.40
f
b
$k_R(\mu m^2 s^{-1})$
0
2
4
6
8
10
12
14
0.10 0.15 0.20 0.25 0.30 0.35 0.40
f
c
$D(\mu m^2/s)$
0.0
0.5
1.0
1.5
0.10 0.15 0.20 0.25 0.30 0.35 0.40
f

FIGURE 4 Effect of the concentration of R (expressed as the fraction of covered area *f*) on the diffusive rate constant k_D (*a*), the reactive rate constant k_R (*b*), and the total diffusion coefficient *D* (*c*) for the monomeric diffusive (*solid black circles*) and dispersed crystals (*red squares*) scenarios. In *open circles* we show results for a configuration where rhodopsin monomers are static and randomly allocated. In (a) and (b) the error bars are ± 2 standard deviations from 3 independent estimations of k_D and k_R. In (c) the error bars are ± 2 standard errors.

In contrast to k_D, the reactive constant k_R is higher in the dispersed crystals configuration compared to the monomeric diffusing scheme (Fig. 4 *b*). This is in agreement with a higher probability of recollision in the former configuration (Fig. 3 *c*). Furthermore, while in the monomeric diffusive system k_R has a weak dependence on the concentration of receptors, in the dispersed crystals organization k_R increases significantly as the levels of R increase (Fig. 4 *b*). To identify effects from the particular organization of the receptors in the dispersed crystals configuration, we compute k_R for the static random configuration of R as well (Fig. 4 *b*, *open circles*). The dispersed crystals configuration shows a higher k_R than the static random scheme, indicating that the organized arrangement of interspersed R dimers results in a higher probability of recollisions between R* and G.

As discussed before, the association rate depends on both the first-encounter rate and the probability of recollisions, and such dependence can be expressed by Eq. (1) via k_D and k_R where it is evident that the collision efficiency *p* modulates the contribution of those factors. When *p* is high, for example, the first-encounter rate is dominant and the association rate constant *k* behaves as k_D (compare Figs. 4 *a* and 5 *a*). In this case the monomeric diffusive system results in higher *k* than the dispersed crystals configuration, and the association rate constant decreases with higher concentration of R in both cases (Figs. 4 *a* and 5 *a*). In contrast, for low collision efficiency, recollisions are more important, and *k* shows a similar behavior as k_R. In this regime, the dispersed crystals configuration results in higher association rates than the monomeric diffusive system. Furthermore, *k* increases with higher levels of R in the dispersed crystals configuration, but remains mostly unchanged in the monomeric diffusive system. (Figs. 4 *b* and 5 *b*).

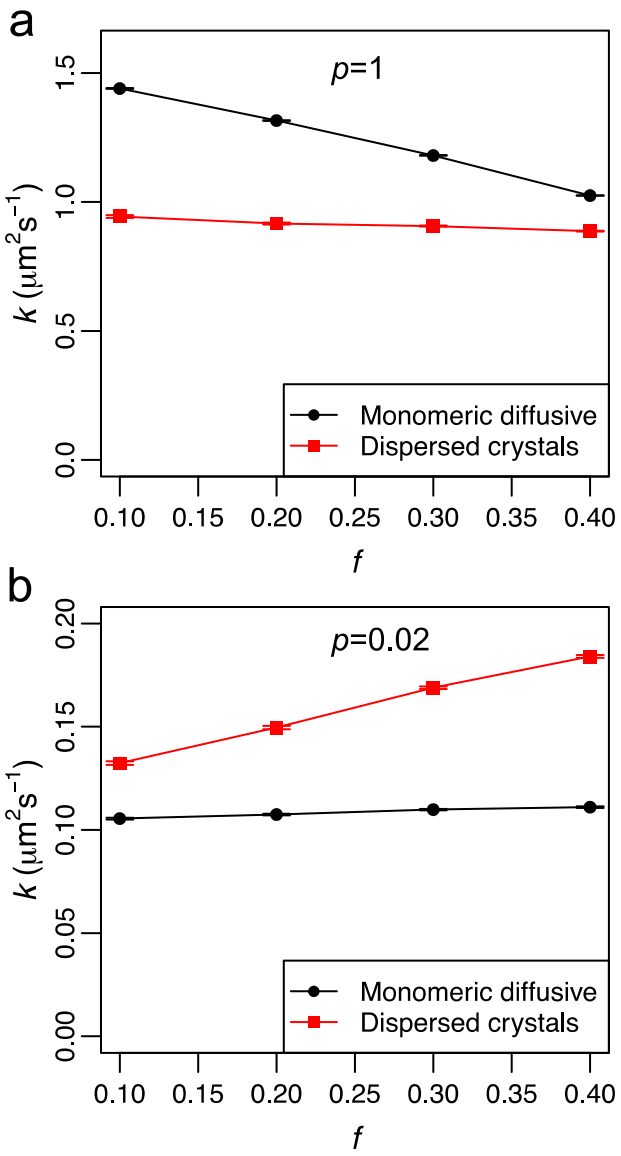

FIGURE 5 The trend of the association rate constant *k* as a function of the concentration of R depends on the collision efficiency. (a) High collision efficiency (p = 1). (b) Low collision efficiency (p = 0.02). Error bars are ± 2 SE.

Lastly, we considered a configuration where rhodopsin is organized in tracks of two adjacent rows of dimers, based on recent observations by Gunkel et al. [10] (Fig. 6A). Surprisingly, this organization yields very similar binding rates compared to the dispersed crystals configuration, showing faster association than the monomeric diffusive scenario for low collision efficiencies, and slower rates than the mobile system for larger values of *p*. These results suggest that the enhanced recollisions that foster binding rates at low *p* are mostly attributed to static receptor

dimers interspaced with free membrane where G can diffuse across, and whether the higher order structures are tracks or dispersed crystals does not have a major impact.

Gunkel et al. 2015 [10] proposed that the tracks organization in combination with transient association of G with inactive R [24,25] can result in trapping of G proteins in the tracks, a phenomenon that they called kinetic trapping. Upon photoactivation of a single rhodopsin, the G proteins trapped in the track containing R* will be activated more rapidly than G proteins coming from other tracks resulting in a biphasic response [10]. We argue that kinetic trapping should be facilitated by recollisions, as repeated encounters between G and R will enhance the formation of non-productive R-G complexes. Furthermore, in such a scenario, G proteins could be enriched in nanodomains and depleted in membrane regions free of rhodopsin, as recollision-enhanced association with R could promote longer residence times of G in areas with high density of R. As our results indicate that recollisions are similar in crystals and tracks configurations, we suggest that kinetic trapping and perhaps G enrichment in nanodomains may be possible in both types of architectures.

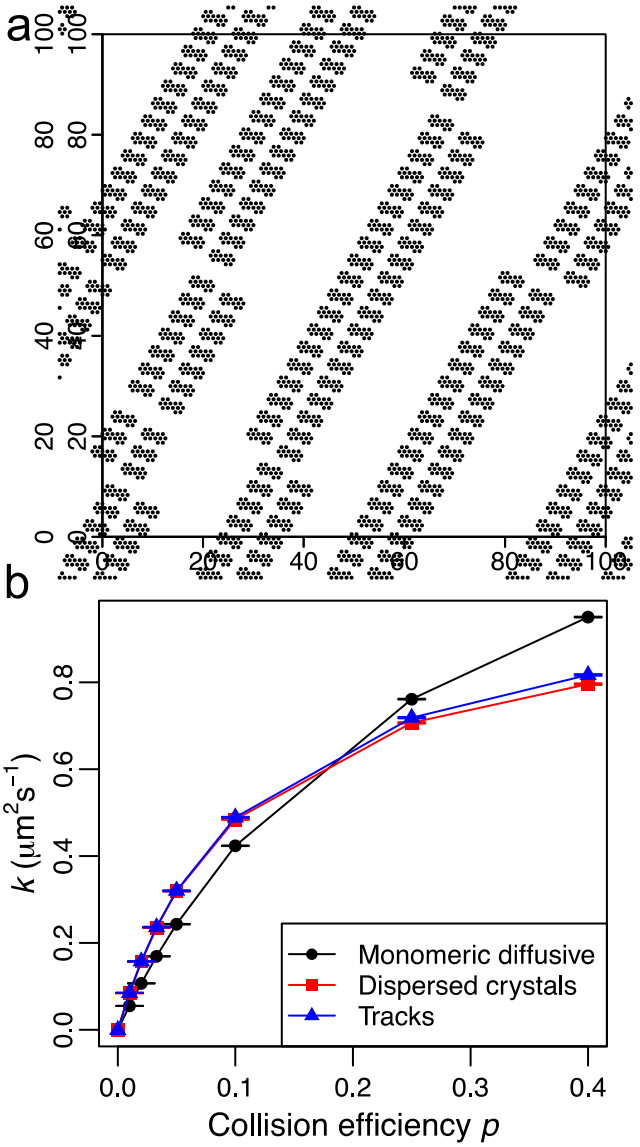

FIGURE 6 An organization where the receptors are arranged in tracks results in similar association rates than the dispersed crystals configuration. (*a*) In the tracks organization, adjacent rows of dimers form "canals" free of receptors. (*b*) Association rate constant *k* for the monomeric diffusive, dispersed crystals and tracks organizations as a function of the collision efficiency *p*. Error bars are ± 2 SE.

Overall, our results suggest that the effect of the configuration of rhodopsin on the association rate between R* and G depends dramatically on the probability of binding upon collision. The

collision efficiency of this reaction is believed to be low [26], therefore, the aggregation of receptors into static ordered configurations may result in a kinetic advantage over a configuration where monomeric R freely diffuses. As we present here, such a kinetic advantage is due to enhanced recollisions between R* and G.

In this work, we considered how the organization of rhodopsin can influence the association reaction between R* and G due to volume exclusion effects. These effects may have further consequences on photon detection [27] by affecting other reactions occurring at the disc membrane, for example, the phosphorylation of R* by rhodopsin kinase, the activation of cGMP phosphodiesterase by activated transducin and deactivation of transducin mediated by RGS proteins [28]. Investigating how the organization of rhodopsin can affect such reactions is a possible extensions of this study. Furthermore, the effects that we study here may be applicable to other GPCR systems where the receptors aggregate forming oligomers in the membrane [29–32].

CONCLUSIONS

By means of Monte Carlo simulations, we studied how different organizations of rhodopsin in the membrane influence the association reaction between a photoactivated receptor and transducin. We considered three plausible scenarios: (a) rhodopsin molecules diffuse on the membrane in monomeric form, (b) the receptors are arranged in static dispersed crystals made of rows of dimers, and (c) rhodopsin molecules are assembled in static tracks made of two adjacent rows of dimers.

The collision efficiency p determines how the configuration of rhodopsin affects the association rate between G and R*. For high p, the association rate is higher in the scenario where rhodopsin molecules diffuse as monomers. However, for low collision efficiencies, k is higher in the structured static configurations. The tracks arrangement and the dispersed crystals configuration result in similar association rates.

Higher concentrations of R will promote recollisions between G and the receptor and can enhance association for low collision efficiencies. This tendency is stronger for configurations

with organized static receptors and is weak for a scenario where R monomers freely diffuse. In a situation with high collision efficiencies (diffusion controlled association), higher levels of R will reduce association rates in general due to slower protein mobility, but this trend is weak for static organized R configurations.

Supporting Information. Simulations varying the number of active sites. Simulations of the tracks configuration varying the track mean length.

ACKNOWLEDGMENTS. We would like to thank Juan Manuel Pedraza for the motivation he provided at the initial stages of this work. This work was supported with funding from the Faculty of Sciences at Universidad de los Andes.

REFERENCES

(1) Rieke, F.; Baylor, D.A. Single-photon detection by rod cells of the retina. Rev. Mod. Phys. 1998, 70, 1027-1036.

(2) Cone, R.A. Rotational diffusion of rhodopsin in the visual receptor membrane. Nat. New Biol. 1972, 236, 39-43.

(3) Poo, M.M.; Cone, R.A. Lateral diffusion of rhodopsin in the photoreceptor membrane. Nature. 1974, 247, 438-441.

(4) Whited, A.M.; Park, P.S.H. Nanodomain organization of rhodopsin in native human and murine rod outer segment disc membranes. Biochim. Biophys. Acta - Biomembr. 2015, 1848, 26-34.

(5) Liang, Y.; Fotiadis, D.; Filipek, S.; Saperstein, D.A.; Palczewski, K.; Engel, A. Organization of the G protein-coupled receptors rhodopsin and opsin in native membranes. J. Biol. Chem. 2003, 278, 21655-21662.

(6) Suda, K; Filipek, S.; Palczewski, K.; Engel, A.; Fotiadis, D. The supramolecular structure of the GPCR rhodopsin in solution and native disc membranes. Mol. Membr. Biol. 2004, 21, 435-446.

(7) Palczewski, K. Oligomeric forms of G protein-coupled receptors (GPCRs). Trends Biochem. Sci. 2010;35:595-600.

(8) Fotiadis, D.; Liang, Y.; Filipek, S.; Saperstein, D.A.; Engel, A.; Palczewski, K. Atomic-Force microscopy: Rhodopsin dimers in native disc membranes. Nature. 2003, 421, 127-128.

(9) Buzhynskyy, N.; Salesse, C.; Scheuring, S. Rhodopsin is spatially heterogeneously distributed in rod outer segment disk membranes. J. Mol. Recognit. 2011, 24, 483-489.

(10) Gunkel, M.; Schöneberg, J.; Alkhaldi, W.; Irsen, S.; Noé, F; Kaupp, U.B; Al-Amoudi, A. Higher-order architecture of rhodopsin in intact photoreceptors and its implication for phototransduction kinetics. Structure. 2015, 23, 628-638.

(11) Govardovskii, V.I.; Korenyak, D.A.; Shukolyukov, S.A.; Zueva, L.V. Lateral diffusion of rhodopsin in photoreceptor membrane: a reappraisal. Mol. Vis. 2009, 15, 1717-1729.

(12) Govardovskii, V.I.; Firsov, M.L. Unknown mechanisms regulating the GPCR signal cascade in vertebrate photoreceptors. Neurosci. Behav. Physiol. 2012, 42, 180-192.

(13) Dell'Orco, D. A physiological role for the supramolecular organization of rhodopsin and transducin in rod photoreceptors. FEBS Lett. 2013, 587, 2060-2066.

(14) Dell'Orco, D.; Schmidt, H. Mesoscopic Monte Carlo simulations of stochastic encounters between photoactivated rhodopsin and transducin in disc membranes. J. Phys. Chem. B. 2008, 112, 4419-4426.

(15) Schöneberg, J.; Heck, M.; Hofmann, K.P.; Noé, F. Explicit spatiotemporal simulation of receptor-G protein coupling in rod cell disk membranes. Biophys. J. 2014, 107, 1042-1053.

(16) Kim, J.S.; Yethiraj, A. Effect of macromolecular crowding on reaction rates: A computational and theoretical study. Biophys. J. 2009, 96, 1333-1340.

(17) Kim, J.S.; Yethiraj, A. Crowding effects on association reactions at membranes. Biophys. J. 2010, 98, 951-958.

(18) Palczewski, K. G protein–coupled receptor rhodopsin. Annu. Rev. Biochem. 2006, 75, 743-

767.

(19) Lambright, D.G.; Sondek, J.; Bohm, A.; Skiba, N.P.; Hamm, H.E.; Sigler, P.B. The 2.0 Å crystal structure of a heterotrimeric G protein. Nature. 1996, 379, 311-319.

(20) Filipek, S.; Krzysko, K.A.; Fotiadis, D; Liang, Y.; Saperstein, D.A.; Engel, A.; Palczewski, K. A concept for G protein activation by G protein-coupled receptor dimers: The transducin/rhodopsin interface. Photochem. Photobiol. Sci. 2004, 3, 628-638.

(21) Wang, Q.; Zhang, X.; Zhang, L.; He, F.; Zhang, G.; Jamrich, M.; Wensel, T. Activation-dependent hindrance of photoreceptor G protein diffusion by lipid microdomains. J. Biol. Chem. 2008, 283, 30015-30024.

(22) Buján-Nuñez, M.C.; Miguel-Fernández, A.; López-Quintela, M.A. Diffusion-influenced controlled reaction in an inhomogeneous medium: Small concentration of reagents. J. Chem. Phys. 2000, 112, 8495-8501.

(23) Saxton, M.J. Anomalous diffusion due to obstacles: a Monte Carlo study. Biophys. J. 1994;66:394-401.

(24) Dell'Orco, D.; Koch, K.W. A dynamic scaffolding mechanism for rhodopsin and transducin interaction in vertebrate vision. Biochem J. 2011;440:263-271.

(25) Fanelli, F.; Dell'Orco, D. Rhodopsin activation follows precoupling with transducin: Inferences from computational analysis. Biochemistry. 2005, 44, 14695-14700.

(26) Kahlert, M.; Hofmann, K.P. Reaction rate and collisional efficiency of the rhodopsin-transducin system in intact retinal rods. Biophys, J. 1991;59:375-386.

(27) Cangiano, L.; Dell'Orco, D. Detecting single photons: A supramolecular matter? FEBS Lett. 2013, 587, 1-4.

(28) Yau, K.W.; Hardie, R.C. Phototransduction motifs and variations. Cell. 2009, 139, 246-264.

(29) Lopez-Gimenez, J.F.; Canals, M.; Pediani, J.D.; Milligan, G. The alpha1b-Adrenoceptor Exists as a Higher-Order Oligomer: Effective oligomerization is required for receptor

maturation, surface delivery, and function. Mol. Pharmacol. 2007, 71, 1015-1029.

(30) Liste, M.J.V.; Caltabiano, G.; Ward, R.J.; Alvarez-Curto, E.; Marsango, S.; Milligan, G. The molecular basis of oligomeric organization of the human M3 muscarinic acetylcholine receptor. Mol. Pharmacol. 2015, 87, 936-953.

(31) Ward, R.J.; Pediani, J.D.; Godin, A.G.; Milligan, G. Regulation of oligomeric organization of the serotonin 5-hydroxytryptamine 2C (5-HT2C) receptor observed by spatial intensity distribution analysis. J. Biol. Chem. 2015, 290, 12844-12857.

(32) Armando, S.; Quoyer, J.; Lukashova, V.; Maiga, A.; Percherancier, Y.; Heveker, N.; Pin, J.P.; Prézeau, L.; Bouvier, M. The chemokine CXC4 and CC2 receptors form homo- and heterooligomers that can engage their signaling G-protein effectors and βarrestin. FASEB J. 2014, 28, 4509-4523.

Table of Contents Graphic (TOC)

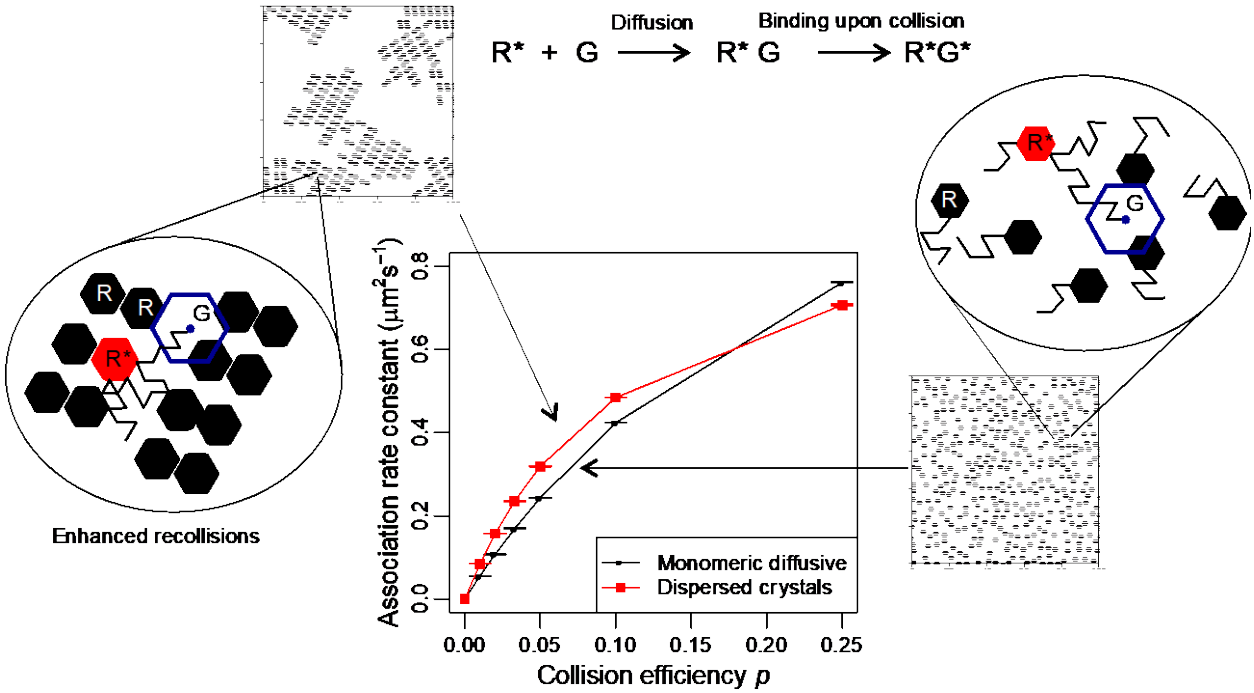
Diffusion
Binding upon collision
R* + G
R* G
R*G*
R
R
G
R*
Enhanced recollisions
Association rate constant (μm²s⁻¹)
0.0
0.2
0.4
0.6
0.8
0.00
0.05
0.10
0.15
0.20
0.25
Collision efficiency p
Monomeric diffusive
Dispersed crystals